Targeting of *HER2*-Expressing Tumors Using ^{111}In-ABY-025, a Second-Generation Affibody Molecule with a Fundamentally Reengineered Scaffold

Sara Ahlgren[1], Anna Orlova[2,3], Helena Wållberg[2], Monika Hansson[2], Mattias Sandström[4], Richard Lewsley[5], Anders Wennborg[2], Lars Abrahmsén[2], Vladimir Tolmachev[1–3], and Joachim Feldwisch[2,3]

[1]Division of Nuclear Medicine, Department of Medical Sciences, Uppsala University, Uppsala, Sweden; [2]Affibody AB, Stockholm, Sweden; [3]Division of Biomedical Radiation Sciences, Department of Radiology, Oncology and Clinical Immunology, Rudbeck Laboratory, Uppsala University, Uppsala, Sweden; [4]Hospital Physics, Department of Oncology, Uppsala University Hospital, Uppsala, Sweden; and [5]Department of Metabolism, Covance Laboratories Ltd., Harrogate, United Kingdom

Overexpression of the human epidermal growth factor receptor type 2 (*HER2*) in breast carcinomas predicts response to trastuzumab therapy. Affibody molecules based on a nonimmunoglobulin scaffold have demonstrated a high potential for in vivo molecular imaging of *HER2*-expressing tumors. The reengineering of the molecular scaffold has led to a second generation of optimized Affibody molecules that have a surface distinctly different from the parental protein domain from staphylococcal protein A. Compared with the parental molecule, the new tracer showed a further increased melting point, stability, and overall hydrophilicity and was more amenable to chemical peptide synthesis. The goal of this study was to assess the potential effects of this extensive reengineering on *HER2* targeting, using ABY-025, a DOTA-conjugated variant of the novel tracer. **Methods:** ^{111}In-ABY-025 was compared with previously evaluated parent *HER2*-binding Affibody tracers in vitro and in vivo. The in vivo behavior was further evaluated in mice bearing SKOV-3 xenografts, rats, and cynomolgus macaques (*Macaca fascicularis*). **Results:** ^{111}In-ABY-025 bound specifically to *HER2* in vitro and in vivo. Direct comparison with the previous generation of *HER2*-binding tracers showed that ABY-025 retained excellent targeting properties. Rapid blood clearance was shown in mice, rats, and macaques. A highly specific tumor uptake of 16.7 ± 2.5 percentage injected activity per gram of tissue was seen at 4 h after injection. The tumor-to-blood ratio was 6.3 at 0.5 h and 88 at 4 h and increased up to 3 d after injection. γ-camera imaging of tumors was already possible at 0.5 h after injection. Furthermore, the repeated intravenous administration of ABY-025 did not induce antibody formation in rats. **Conclusion:** The biodistribution of ^{111}In-ABY-025 was in remarkably good agreement with the parent tracers, despite profound reengineering of the nonbinding surface. The molecule displayed rapid blood clearance in all species investigated and excellent targeting capacity in tumor-bearing mice, leading to high tumor-to-organ-ratios and high-contrast imaging shortly after injection.

Key Words: molecular imaging; peptides; radiopharmaceuticals; Affibody molecule; reengineered scaffold

J Nucl Med 2010; 51:1131–1138
DOI: 10.2967/jnumed.109.073346

Malignant transformation of cells is often associated with genotypic and phenotypic changes, such as overexpression of certain receptors. With the emergence of targeted therapies and personalized medicine, detection of specific receptors has become increasingly important as molecular signatures of cancer. One such receptor is the human epidermal growth factor receptor type 2 (*HER2*) belonging to the receptor tyrosine kinase superfamily (*1*). Overexpression of *HER2* is found in a variety of cancers—for example, breast, ovary, colorectal, and urothelial carcinomas—and is associated with a more aggressive disease and poor prognosis (*1*). *HER2* is the target for a variety of established and novel therapeutic approaches, including monoclonal antibodies, antibody–drug conjugates, and small molecules (*2*). Clinical practice guidelines of the American Society of Clinical Oncology and European Group on Tumor Markers recommend the assessment of *HER2* expression in all newly diagnosed or recurrent breast carcinomas to select patients who will benefit from treatment with trastuzumab and anthracyclines (*3,4*). A molecular imaging agent for in vivo detection of this target could therefore have clinical use for predicting treatment effect. The main advantage of radionuclide tumor targeting for visualization of *HER2*, over the current methods based on tissue samples, is the ability of this method to avoid the pitfalls of biopsy-based detection, including sampling errors, and discordance in biomarker

Received Dec. 1, 2009; revision accepted Mar. 17, 2010.
For correspondence or reprints contact: Vladimir Tolmachev, Division of Biomedical Radiation Sciences, Rudbeck Laboratory, Uppsala University, SE-751 85, Uppsala, Sweden.
E-mail: Vladimir.Tolmachev@bms.uu.se

expression in primary tumors and metastases (*5*). An important prerequisite for this application is the high sensitivity and specificity for *HER2* expression.

A general problem with full-size antibodies as tracers for molecular imaging is a low sensitivity and reduced contrast of imaging, because of the long residence time in blood causing high background activity (*6*). The analysis of preclinical data has shown that smaller tracers, associated with a shorter residence time in blood, may provide better imaging contrast and therefore superior sensitivity (*7*). Calculations based on experimental biodistribution data suggest that a tracer should be as small as possible, not just below the threshold for kidney clearance (*8*). Thus, sizes below what is achievable with the smallest antibody fragments should provide favorable contrast, arguing for the use of nonimmunoglobulin-based scaffolds for making tracers. One such class of tracers is Affibody molecules (Affibody AB), or scip (Affibody AB), made on a scaffold from a 6.5-kDa 3-helical bundle Z domain derived from staphylococcal protein A (*9,10*). The Affibody molecule $Z_{HER2:342}$, binding the extracellular domain of *HER2* with high affinity (K_D, 22 pM), was recently developed (*11*). Clinical imaging of *HER2*-expressing metastases using ^{111}In- and ^{68}Ga-labeled variants of this molecule has been demonstrated (*12*).

The Z domain is an engineered protein A domain that—because of the replacement G29A—interacts weakly with the variable domain of antibodies of the variable heavy-chain 3 family. Affibody molecule libraries have been generated by randomization of 13 surface-exposed residues of the Z domain, whereby the antibody Fc binding capability was replaced with the potential to bind other targets (*13*). The most studied Affibody molecules are variants of the *HER2*-binding $Z_{HER2:342}$. Preclinical data have shown that tracers based on this molecule can detect the in vivo decrease of *HER2* expression in response to inhibition of its chaperone heat shock protein 90, indicating utility for therapy monitoring (*14,15*). Notably, the tracer does not compete with trastuzumab for the same binding site on *HER2* (*14,16*) and should therefore enable discrimination between receptor blocking and receptor downregulation in analogy to pertuzumab, recently used for monitoring the effect of trastuzumab therapy (*17*). Different Affibody molecules have been shown to yield high-contrast imaging in several preclinical studies, with alternative labeling chemistry and isotopes, including iodine (*11,16*), bromine (*18*), fluorine (*15*), and indium in combination with different chelators (*14,19–21*). The effect of alternative N termini on labeling with ^{99m}Tc and biodistribution properties was investigated in a series of experiments (*22*). Small changes in the amino-terminal end of the tracer protein resulted in widely different biodistribution properties, with more hydrophilic molecules displaying a lower degree of undesirable hepatobiliary excretion.

Recently, an optimized *HER2*-binding Affibody molecule was made by reengineering the nonbinding surface of $Z_{HER2:342}$ to make it distinctly different from any protein A domain (*23*). Several aspects of the protein were improved, including amenability for peptide synthesis, storage stability (avoiding deamidation), increased melting point, and surface hydrophilicity. In the resulting $Z_{HER2:2891}$, compared with the original $Z_{HER2:342}$, as many as 11 surface-accessible amino acid residues were changed (*11*). A DOTA moiety, denoted ABY-025, was site-specifically conjugated at a unique C-terminal cysteine to create a novel tracer for molecular imaging of *HER2*-expressing tumors. The primary goal of this study was to assess the potential effects of these extensive amino acid replacements on the properties influencing in vivo *HER2* detection accuracy, particularly uptake in tumors and healthy tissues. To achieve this goal, ABY-025 was compared with 2 variants of its precursor. Cell-binding properties, biodistribution, and tumor targeting in mouse xenografts are investigated. The secondary goal was to investigate pharmacokinetics in rats and macaques (*Macaca fascicularis*) and immunogenicity in rats in preparation for potential clinical development.

MATERIALS AND METHODS

Materials

^{111}In-chloride was purchased from Covidien (DRN 4901). Maleimide-DOTA was purchased from Macrocyclics. DOTA-$Z_{HER2:342\text{-}pep2}$ was made by standard Fmoc solid-phase peptide synthesis in a single chemical process by Bachem as described by Orlova et al. (*14*). The Affibody molecules $Z_{HER2:2891}$-Cys, $Z_{HER2:2395}$-Cys, and $Z_{Taq:3638}$-Cys, all having a unique cysteine at the C terminus, were produced in Escherichia *coli* and purified as described earlier (*21*). Data on cellular uptake, biodistribution, and γ-camera images were analyzed by unpaired, 2-tailed *t* test using GraphPad Prism (version 4.00 for Windows [Microsoft]; GraphPad Software) to determine significant differences ($P < 0.05$).

Instrumentation

Radioactivity was detected with an automated γ-counter with a NaI(Tl) detector (1480 Wizard [Wallac Oy] and Cobra II [Packard]). The Cyclone Storage Phosphor System and OptiQuant image-analysis software (Perkin-Elmer) were used to measure the radioactivity on the instant thin-layer chromatography strips. The Affibody molecules were analyzed by high-performance liquid chromatography and online mass spectrometry, as described by Ahlgren et al. (*21*).

Conjugation and Labeling Chemistry

The recombinantly produced Affibody molecules were conjugated with maleimide-DOTA as described earlier (*21*). The resulting molecules were designated as ABY-025 ([maleimide-DOTA-Cys^{61}]-$Z_{HER2:2891}$-Cys; DOTA-$Z_{HER2:2891}$-C), DOTA-$Z_{HER2:2395}$-C ([maleimide-DOTA-Cys^{61}]-$Z_{HER2:2395}$-Cys), and DOTA-Z_{taq}-C ([maleimide-DOTA-Cys^{61}]-$Z_{Taq:3638}$-Cys). Labeling was performed by mixing 50 μg of DOTA-conjugated Affibody molecule (1 μg/μL) in 1 M ammonium acetate buffer, pH 5.5, with a predetermined amount of ^{111}In in 0.05 M HCl and incubating for 30 min at 60°C. ^{111}In-ABY-025 was analyzed using size-exclusion chromatography to confirm the absence of aggregates (Supplemental Fig. 1; supplemental materials are available online only at http://jnm.snmjournals.org). For cell studies and biodistribution experiments, the sample was diluted with phosphate-buffered saline.

In Vitro Characterization

The in vitro binding specificity of ^{111}In-labeled *HER2*-binding Affibody molecules was assessed in *HER2*-expressing human ovarian adenocarcinoma SKOV-3 cells (HTB-77; American Type Culture Collection [ATCC]) by receptor presaturation with unlabeled *HER2*-binding tracer as described by Ahlgren et al. (*21*). The binding specificity of ^{111}In-ABY-025 was confirmed in 2 other *HER2*-expressing cell lines: human mammary gland carcinoma SKBR-3 (HTB-30; ATCC) and human gastric carcinoma NCI-N87 (CRL-5822; ATCC). Cellular retention and internalization of radioactivity was evaluated as described by Ahlgren et al. (*21*) using these 3 cell lines. The antigen-binding capacity of ^{111}In-ABY-025 (for antibodies often referred to as the immunocompetent fraction) was determined using SKOV-3 cells, according to procedures described by Lindmo et al. (*24*) and Engfeldt et al. (*25*).

In Vivo Experiments

All animal experiments were planned and performed in accordance with the respective national legislation on laboratory animals, and the animal study plans were approved by the local Ethics Committees for Animal Research.

BALB/c *nu/nu* mice were purchased from Taconic. The tumor model was obtained by subcutaneously implanting 10^7 *HER2*-expressing SKOV-3 cells into the right hind leg. Control mice were implanted with a similar amount of the non–*HER2*-expressing A431 cells (CRL-1555; ATCC). At the time of the biodistribution experiment, the average tumor weight was 250 ± 98 mg.

In the biodistribution experiments, mice bearing *HER2*-expressing tumors were randomized into groups of 4 and injected intravenously with 1 μg of conjugate (30 kBq) in 100 μL of phosphate-buffered saline. The radiochemical purity of radiolabeled conjugates used in the animal experiments exceeded 97%. Mice were euthanized by anesthesia overdosing at predesignated time points. Blood was collected by heart puncture. Organ samples were collected in preweighed plastic vials. All tissue radioactivity uptake values were calculated as percentage of injected activity per gram of tissue (%IA/g), except for the thyroid, gastrointestinal tract, and carcass, for which the uptake was calculated as %IA per whole sample. The radioactivity in the gastrointestinal tract with its content was used as a measure of hepatobiliary excretion. The specificity of *HER2* targeting in mice bearing SKOV-3 xenografts was assessed by presaturating *HER2* receptors with 600 μg of unlabeled His_6-$Z_{HER2:342}$ subcutaneously injected 45 min before injection of ^{111}In-ABY-025.

For γ-camera imaging, 4 animals were injected with 4.5 MBq of ^{111}In-ABY-025 (1.5 MBq/μg). The mice were euthanized by overdosing with ketamine (Ketalar; Parke Davis)/xylazine (Rompun; Bayer AG) at 0.5 or 4 h after injection. After euthanasia, the urinary bladders were dissected. Imaging was performed using a Millennium VG γ-camera (GE Healthcare) equipped with a medium-energy general-purpose collimator. Static images (10 min) were obtained with a zoom factor of 2.0 and digitally stored in a 256 × 256 matrix. ^{111}In was measured using a summation of both photopeaks (energy settings centered around 171 and 245 keV, respectively, ±10%). Images were evaluated using Osiris 4.19 software (Digital Imaging Group). In each animal, a region of interest was drawn around the tumor. The same region was copied to a contralateral thigh. Tumor–to–contralateral thigh ratios were calculated on the basis of total counts in the regions of interest.

The immunogenicity study was done using female outbred Sprague–Dawley rats (Scanbur AB), 8–12 wk old at the start of the experiment. The animals were randomly assigned to 3 groups of 8. The rats in each group received intravenous injections with ABY-025 (2, 6, or 20 μg) on days 0, 21, 42, 63, and 84. Blood samples were collected on days −1 (preserum), 20, 41, 62, 83, and 94. Serum was prepared, and the samples were stored at −20°C until analysis.

Serum samples were subjected to a 2-tier analysis in an antidrug antibody enzyme-linked immunosorbent assay (ELISA). First, samples positive for anti-ABY-025 antibodies were identified in a screening assay; then, positive samples were subjected to a confirmatory assay for which the specificity for ABY-025 was determined. Briefly, ELISA plates were coated with 1 μg of ABY-025 per milliliter in carbonate buffer (Sigma-Aldrich). Rat serum samples and positive controls were added in duplicates to the plates, at the minimum dilution of 1 in 100. As the secondary antibody, peroxidase-conjugated goat antirat IgG (Southern Biotechnology Inc.) at a dilution of 1 in 6,000 was used, and the substrate was TMB ImmunoPure (Pierce). The absorbance at 450 nm was measured using a Victor^3 ELISA reader (Perkin-Elmer). The confirmatory assay was similar to the screening assay, with the exception that the samples were diluted either in buffer only or in buffer containing 1 μg of ABY-025 per milliliter and preincubated for 30 min before analysis. Samples with at least a 30% reduction in absorbance value when mixed with ABY-025, compared with buffer, were considered to contain antibodies specific for ABY-025.

Pharmacokinetic studies were performed in outbred Wistar (Han) rats from Charles River Ltd. and macaques from Bioculture Co. Ltd. or Bioda Co. Ltd. (Mitius) as described in the supplemental materials.

RESULTS

Conjugation and Labeling Chemistry

Liquid chromatography–mass spectrometry analysis showed no unconjugated $Z_{HER2:2891}$-Cys after conjugation with maleimide-DOTA at a chelator-to-protein molar ratio of 3:1. It was previously shown that the affinity for *HER2* was similar with or without the DOTA moiety (K_D values, 60 pM and 76 pM, respectively) (*23*). Incubation of ABY-025 with ^{111}In at 60°C during 30 min repeatedly provided more than 95% incorporated ^{111}In ($n > 20$, data not shown). A specific radioactivity of 15.1 GBq/μmol (2 MBq/μg) was obtained. Size-exclusion chromatography confirmed that all radioactivity was associated with a peak having the same retention time as the monomeric control Affibody molecule (Supplemental Fig. 1). For biologic experiments, all conjugates were used without further purification.

In Vitro Characterization

ABY-025 was compared with 2 variants of the parent *HER2*-binding Affibody molecule, DOTA-$Z_{HER2:342\text{-}pep2}$ and DOTA-$Z_{HER2:2395}$-C. DOTA-$Z_{HER2:342\text{-}pep2}$ can be produced only by peptide synthesis, whereas DOTA-$Z_{HER2:2395}$-C is preferably made recombinantly. The differences in amino acid sequence are shown in Figure 1.

HER2 specificity was assessed in a blocking experiment. Saturation of *HER2* receptors using nonlabeled *HER2*-binding tracer before incubation with ^{111}In-ABY-025 for 1 h at 37°C reduced the cell-bound radioactivity from 34% ±

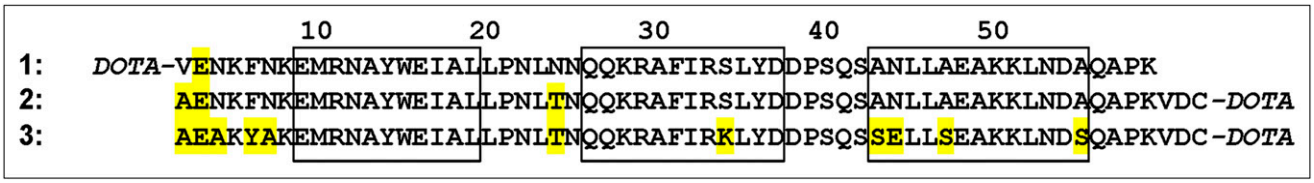

FIGURE 1. Alignment of studied *HER2*-binding Affibody molecules. Three molecules are denoted: 1, DOTA-$Z_{HER2:342\text{-}pep2}$; 2, DOTA-$Z_{HER2:2395}$-C; and 3, ABY-025. Approximate positions of α-helices 1 through 3 are indicated by boxes. Eleven amino acids in $Z_{HER2:2891}$ sequence that were replaced in comparison to original $Z_{HER2:342}$ are highlighted by yellow background in each of the 3 sequences. DOTA chelators are indicated in italics. $Z_{HER2:342}$-variant used in present study was improved for peptide synthesis by replacement of aspartate in position 2 for glutamate.

5% to 1.6% ± 0.4% ($P < 0.001$) for SKOV-3 cells, from 38% ± 2% to 1.6% ± 0.4% ($P < 10^{-5}$) for SKBR-3 cells, and from 36 ± 1 to 2.22 ± 0.03 for NCI-N87 cells ($P < 10^{-6}$). Similarly, presaturation of *HER2* receptors on SKOV-3 cells reduced binding of ^{111}In-DOTA-$Z_{HER2:2395}$-C and ^{111}In-DOTA-$Z_{HER2:342\text{-}pep2}$ from 42% ± 2% to 1.3% ± 0.3% ($P < 10^{-5}$) and from 41% ± 2% to 1.6% ± 0.7% ($P < 10^{-5}$), respectively. Thus, in each case the binding to *HER2*-expressing cells was *HER2*-specific.

Two alternative methods showed that ^{111}In-ABY-025 displayed an antigen-binding capacity of more than 89%: 89.2% ± 0.6% according to the method of Lindmo et al. (*24*) and 89.8% ± 0.5% according to the method of Engfeldt et al. (*25*) (Supplemental Fig. 2).

The cellular retention of ^{111}In-ABY-025 was excellent. As much as 81% ± 2% of the radioactivity was cell-associated at 24 h after interrupted incubation of SKOV-3 cells with ^{111}In-ABY-025 (Fig. 2). The internalization was relatively slow, showing less than 12% internalized radioactivity after 24 h. The cellular retention pattern was similar in NCI-N87 cells, showing 76% ± 1% cell-associated and 13% ± 1% internalized radioactivity after 24 h at 37°C. With SKBR-3 cells, the cell-associated radioactivity was 58% ± 1%, indicating a slightly lower efficiency of cellular retention. ^{111}In-ABY-025 internalized into SKBR-3 cells more slowly than it did into the cells from the other 2 lines, with only less than 2.5% internalized radioactivity after 24 h. With SKOV-3 and NCI-N87 cells, most of the radioconjugate release occurred within the first hour of incubation, and cell-associated radioactivity remained essentially constant between 2 and 24 h.

In Vivo Experiments

The biodistribution of ^{111}In-ABY-025 in mice bearing SKOV-3 xenografts was compared with that of ^{111}In-DOTA-$Z_{HER2:2395}$-C and ^{111}In-DOTA-$Z_{HER2:342\text{-}pep2}$. The biodistribution pattern of ^{111}In-ABY-025 was similar to that of the parent tracers and characterized by high tumor targeting and low uptake in nonspecific organs, except the expected uptake in the kidneys (Table 1).

A tumor-targeting and biodistribution kinetics study of ^{111}In-ABY-025 was performed in mice bearing SKOV-3 xenografts. Tumor uptake already was prominent (13 ± 2 %IA/g) by 0.5 h after injection and remained as high as 11 ± 4 %IA/g after 24 h (Fig. 3A). A rapid blood clearance resulted in a tumor-to-blood ratio of 6 ± 1 at 1 h after injection, increasing to 88 ± 15 three h later (Supplemental Table 2). The concentration of radioactivity was low in all other organs and tissues, except for the kidneys. Generally, tumor-to-organ ratios increased over time because of a more rapid decrease of radioactivity in nonspecific organs, again with the exception of the kidneys (Fig. 3B). The tumor-to-kidney ratio (not included in Fig. 3B) was 0.09 ± 0.02 at 4 h after injection. Numeric data of the biodistribution and tumor-to-organ ratios are found in Supplemental Tables 1 and 2.

The in vivo *HER2* specificity of tumor binding was assessed in 2 ways (Fig. 4). Two groups of SKOV-3

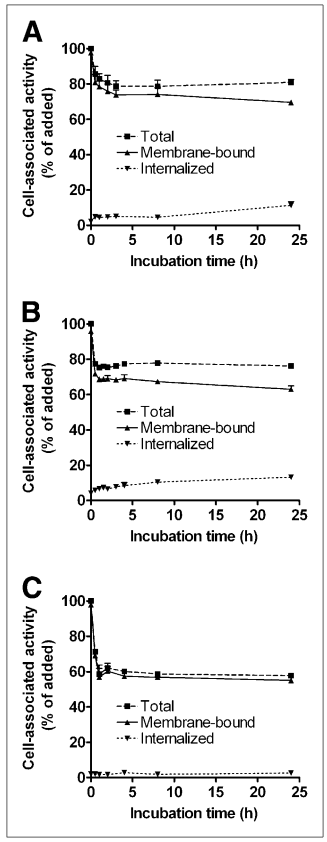

FIGURE 2. Cell-associated radioactivity as function of time. Cells were incubated with ^{111}In-ABY-025 at 4°C and washed before onset of experiment. Cell-associated radioactivity at time zero was set to 100%. Total and cell-bound radioactivity was measured at indicated time points. Radioactivity removed from cells by treatment with 4 M urea solution in 0.2 M glycine buffer, pH 2.0, was considered to be membrane-bound, and remaining radioactivity as internalized. Study was performed on 3 different *HER2*-expressing cell lines: SKOV-3 (A), NCI-N87 (B), and SKBR-3 (C). Data are presented as mean ± SD ($n = 3$). Error bars are not always visible, because they are smaller than symbols in plot.

TABLE 1. Comparative Biodistribution of ^{111}In-ABY-025, ^{111}In-DOTA-$Z_{HER2:2395}$-C, and ^{111}In-DOTA-$Z_{HER2:342\text{-}pep2}$ in BALB/c *nu/nu* Mice Bearing SKOV-3 Xenografts 4 Hours After Injection

Tissue	Uptake (%IA/g) ^{111}In-ABY-025	^{111}In-DOTA-$Z_{HER2:2395}$-C	^{111}In-DOTA-$Z_{HER2:342\text{-}pep2}$
Blood	0.21 ± 0.03	0.19 ± 0.05	0.11 ± 0.03
Lung	0.4 ± 0.2	0.4 ± 0.1	0.3 ± 0.1
Liver	1.7 ± 0.7	1.5 ± 0.3	1.7 ± 0.3
Spleen	0.5 ± 0.2	0.4 ± 0.1	0.49 ± 0.07
Colon	0.3 ± 0.1	0.25 ± 0.04	0.19 ± 0.05
Kidney	184 ± 48	181 ± 17	184 ± 20
Tumor	11 ± 3	11 ± 2	14 ± 1
Muscle	0.10 ± 0.04	0.07 ± 0.01	0.07 ± 0.01
Bone	0.3 ± 0.1	0.20 ± 0.05	0.22 ± 0.08
Gastrointestinal tract†	0.93 ± 0.08	1.8 ± 0.8	0.8 ± 0.2
Carcass	4 ± 1	3.2 ± 0.5	2.5 ± 0.4

Data are presented as average from 4 animals ± SD. Uptake is calculated as %IA/g. Data for gastrointestinal tract (with its content) and carcass are presented as %IA per whole sample.

xenografted mice were injected with ^{111}In-ABY-025 or the non–*HER2*-binding control Affibody molecule ^{111}In-DOTA-Z_{Taq}-C. The tumor uptake of control tracer (0.3 ± 0.1 %IA/g) was much lower at 1 h after injection than uptake of ^{111}In-ABY-025 (17 ± 3 %IA/g; $P < 10^{-4}$). A third group of mice was injected with excess nonlabeled *HER2*-binding Affibody molecule to saturate the *HER2* receptors before administration of ^{111}In-ABY-025, leading to a more than 6-fold decrease in tumor uptake of radioactivity (2.4 ± 0.2 %IA/g, $P < 10^{-4}$).

γ-camera images acquired at 0.5 and 4 h after intravenous injection of ^{111}In-ABY-025 in nude mice bearing SKOV-3 xenografts confirmed that tumor visualization was already feasible at 0.5 h after injection (Fig. 5). The kidneys are clearly seen in the images, because of the renal route of elimination. Rapid clearance from blood and nonspecific organs allowed for increasing contrast at the later time point (4 h after injection). In SKOV-3 xenografted mice, the tumor–to–contralateral thigh ratio was 7 ± 1 (average ± maximum error) at 0.5 h and 25 ± 12 at 4 h after injection. The uptake in *HER2*-negative A431 xenografts was not visible, that is, much lower than that in *HER2*-expressing xenografts.

To assess the immunogenicity, female Sprague–Dawley rats received 5 injections at an interval of 3 wk, mimicking a potential repeated administration in molecular imaging. Three different dose levels were used corresponding (in mg/kg) to 5.6, 29.4, and 56 times the 100-μg dose of DOTA-$Z_{HER2:342\text{-}pep2}$ that was used to obtain clinical PET and SPECT data in breast cancer patients (*12*). No scaling factor was used because the dose was injected intravenously and clearance had been almost entirely renal, with a short expected half-life in mice, rats, and macaques. The occurrence of antibodies binding to ABY-025 was assessed 3 wk

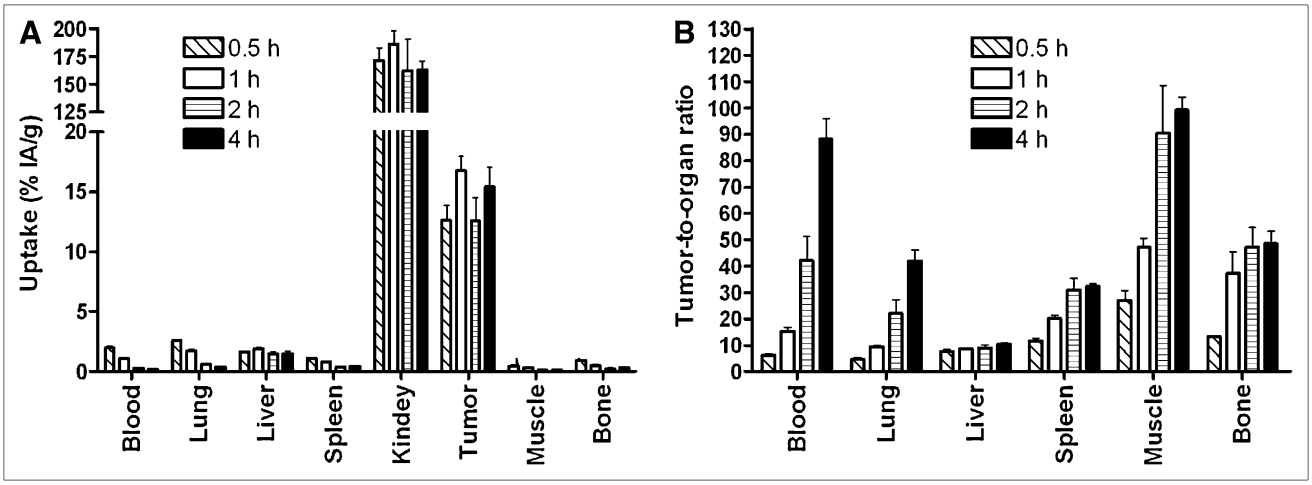

FIGURE 3. Biodistribution expressed as %IA/g (A) and tumor-to-organ ratios (B) of ^{111}In-ABY-025 in BALB/C *nu/nu* mice bearing SKOV-3 xenografts. Data are presented as average from 4 animals ± SD.

TABLE 2. Frequency of Specific Anti-ABY-025 Antibodies

Group	Dose (μg)	No. of animals per dose group	Interval (d)					
			−1	20	41	62	83	94
1	2	8	0	0	1	1	1	1
2	6	8	0	0	0	0	0	0
3	20	8	0	0	0	0	0	0

Animals received 5 consecutive doses at intervals of 21 d. Blood samples were collected on day preceding next injection.

after each injection. The ELISA analysis showed no specific antibodies in 23 of 24 animals, irrespective of dose (Table 2). However, specific antibodies were observed in 1 animal in the lowest dosing group after the second injection. The antibody level was of low magnitude, just above the assay cut point, and not affected by 3 additional injections.

Pharmacokinetic data for rats and macaques are presented in the supplemental materials.

DISCUSSION

The *HER2*-binding ABY-025 based on the second-generation Affibody molecule scaffold was shown to display a higher melting temperature than the parent molecule and the same reversible folding properties (*23*). These data suggested that ABY-025 would tolerate the conditions used during labeling with ^{111}In, an assumption that was confirmed in the present study. Size-exclusion chromatography confirmed that ^{111}In-ABY-025 was monomeric and

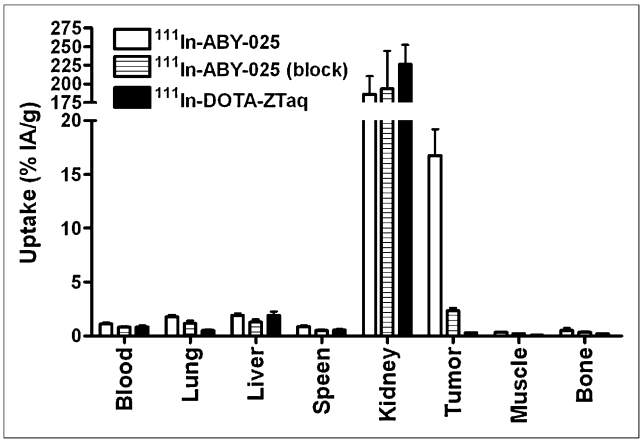

FIGURE 4. Assessment of *HER2* specificity of ^{111}In-ABY-025 tumor uptake in SKOV-3 xenografts. To saturate *HER2* receptors in tumors, 1 group of animals was preinjected with 600 μg of nonlabeled His_6-$Z_{HER2:342}$ 45 min before injection of radiolabeled conjugate. As another negative control, 1 group was injected with non–*HER2*-binding ^{111}In-DOTA-Z_{Taq}-C. All animals were injected with 1 μg of tracer. Data are presented as average from 4 animals ± SD.

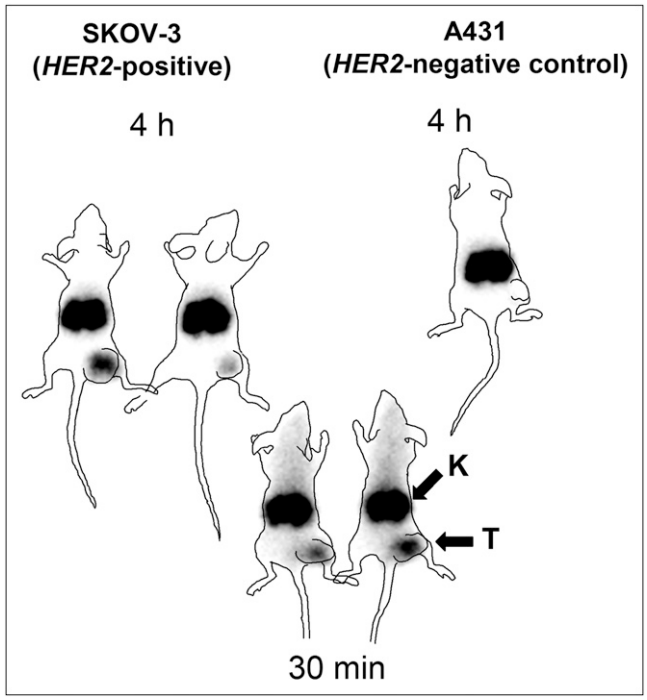

FIGURE 5. Imaging of *HER2* expression in SKOV-3 or A431 xenografted BALB/c *nu/nu* mice. A431 tumors were used as negative control. Planar γ-images were acquired at 30 min and 4 h after administration of ^{111}In-ABY-025 for mice bearing SKOV-3 xenografts and at 4 h for mouse bearing A431 xenografts. Tumors (right hind leg) were visualized only in SKOV-3 xenografts, indicating specific *HER2* binding of ^{111}In-ABY-025. To facilitate interpretation, animal contours were derived from digital photograph and superimposed over γ-camera image. Arrows show tumor (T) and kidneys (K) in 1 representative animal.

not aggregated (Supplemental Fig. 1). The labeled tracer retained its antigen-binding capacity, as shown by *HER2* binding in cellular assays. Furthermore, the specificity of ^{111}In-ABY-025 was confirmed in vitro using several *HER2*-expressing cell lines by blocking with excess unlabeled *HER2*-binding Affibody molecule. The tracer was efficiently retained on *HER2*-expressing cell lines, especially the highly expressing SKOV-3 and NCI-N87 cell lines (Fig. 2). The good retention was mainly due to strong receptor binding rather than internalization and trapping of the radionuclide. These cellular retention data for the reengineered *HER2*-binding tracer ABY-025 are similar to those previously reported for the parental ^{111}In-DOTA-$Z_{HER2:2395}$-C (*21*), ^{99m}Tc-$Z_{HER2:2395}$-C (*26*), and ^{111}In-DOTA-$Z_{HER2:342\text{-}pep2}$ (*27*).

One of the new features of ABY-025 is that it can be produced both by peptide synthesis and in *E. coli* (*23*). In the present study, ^{111}In-ABY-025 was compared with 2 parent *HER2*-binding Affibody molecules—that is, DOTA-$Z_{HER2:342\text{-}pep2}$, which can be produced only by peptide synthesis, and DOTA-$Z_{HER2:2395}$-C, which is less suitable for peptide synthesis and is therefore preferably made recombinantly. Retained *HER2* binding and reduced un-

specific binding to immunoglobulins has been assessed during the engineering program (*23*). As many as 11 of the 45 amino acids common to all original Affibody molecules have been substituted, and all were surface-exposed. Despite these profound changes, the biodistribution pattern of ^{111}In-ABY-025 in mice bearing SKOV-3 xenografts was in remarkable agreement with the 2 parental tracers (Table 1). Previous data showed that even a single substitution could alter the biodistribution pattern dramatically. In the most unfavorable cases, a single amino acid substitution resulted in high liver uptake and hepatobiliary clearance, aggravating high-contrast imaging of tumors and metastases in the abdominal area (*22*). ^{111}In-ABY-025 displayed not only rapid blood clearance in mice (Fig. 4; Supplemental Table 1) but also similar clearance in rats and macaques (Supplemental Fig. 3). Thus, data from 3 species indicate that ABY-025 does not display undesirable binding to plasma proteins or weak unspecific interactions in normal tissues, leading to slow release. This rapid blood clearance is a prerequisite for obtaining a high contrast in molecular imaging studies within hours after administration.

The presence of antibodies specific for the tracer may neutralize the binding to *HER2* receptors and thus result in false-negative results during imaging and alter blood clearance of the tracer. In an effort to study the immunogenic properties of ABY-025, rats received 5 consecutive doses of ABY-025, administered every 3 wk to allow the development of an immune response (Table 2). No specific antibodies against ABY-025 were found in the sera from 23 of 24 animals. However, a low amount was detected in sera from 1 animal in the lowest dosing group, although 3 additional administrations of ABY-025 did not increase the antibody level. This low amount indicates that factors other than treatment may have caused cross-reacting antibodies in this particular individual and suggests that ABY-025 is not immunogenic at these doses. After daily dosing for 14 d, no ABY-025–specific antibodies were detected in any animal in a good laboratory practice toxicity study performed in rats, further supporting that ABY-025 is not immunogenic (data not shown). These data are favorable, although immunogenicity studies in animals have limited predictive value for the human situation. A reliable assessment of immunogenicity can be obtained only from phase III clinical studies, when a larger number of humans have been administered the compound.

^{111}In-ABY-025 showed rapid tumor targeting and low uptake in nontargeted organs and tissues except the kidneys (Fig. 4; Supplemental Table 1). The high renal accumulation has previously been seen both with Affibody molecules and with other small targeting proteins (<60 kDa) and is due to reabsorption in the proximal tubules (*28*). This effect is enhanced by the residualizing properties of radiometals, such as ^{111}In. However, the kidneys are spatially well separated from main metastatic sites of breast cancer, allowing visualization of tumors using SPECT without interference from accumulated renal radioactivity. Nonbound tracer was efficiently cleared from the bloodstream, resulting in a high and increasing tumor-to-nontumor ratio relative to all tissues except the liver, remaining constant at around 10 (Supplemental Table 2). This rapid clearance from the bloodstream allowed for high-contrast imaging by as little as 0.5 h after injection. The image contrast was further increased at 4 h after injection (Fig. 5). Such high contrast should result in high sensitivity of *HER2* imaging in a clinical setting.

The in vivo specificity was confirmed by a blocking experiment, in which the presaturation of *HER2* receptors reduced the tumor accumulation of ABY-025 (Fig. 4). The low accumulation in SKOV-3 tumors of the non–*HER2*-binding ^{111}In-DOTA-Z_{Taq}-C (0.3 ± 0.1 %IA/g—that is, 1.7% of the tumor uptake seen with ^{111}In-ABY-025) demonstrates that tumor targeting was *HER2*-specific. This finding is concordant with the low nonspecific tumor accumulation of other variants of the first generation of *HER2*-binding Affibody molecules (*14,21*). The high specificity of ^{111}In-ABY-025 is remarkable as compared with data on radiolabeled trastuzumab or Fab fragments derived from this monoclonal antibody (*29–32*). In those studies, the uptake of tracers in *HER2*-negative xenografts was 20%−30% of the uptake in *HER2*-positive xenografts. Uptake of nonspecific control antibodies in *HER2*-specific xenografts was also 20%−30% of uptake of *HER2*-specific antibodies. Here the well-known unspecific accumulation of macromolecules in tumors (*33*) could lead to false-positive *HER2*-prediction, whereas the *HER2* tracers based on the Affibody scaffold display appreciably higher molecular specificity. Thus, ^{111}In-ABY-025 provides both high tumor-to-organ ratios (sensitivity) and high specificity, leading to high molecular imaging accuracy.

CONCLUSION

This study confirmed that the ^{111}In-ABY-025 biodistribution pattern agrees well with the radiolabeled variants of the parental *HER2*-binding Affibody molecule, despite profound reengineering of the nonbinding surface of $Z_{HER2:342}$ (19% of the amino acid residues replaced). ABY-025 showed high and specific targeting capacity to *HER2* both in vitro and in vivo, with rapid blood clearance, leading to high tumor-to-organ ratios. A clear and specific visualization of *HER2* expression in a murine xenograft model using ^{111}In-ABY-025 was possible within a few hours after injection. Furthermore, the molecule displayed a rapid blood clearance in rats and macaques and did not induce antibody responses in rats, suggesting that the molecule is suitable for further development.

ACKNOWLEDGMENTS

This research was supported in part by grants from the Swedish Cancer Society (Cancerfonden), Swedish Research Council (Vetenskapsrådet), and the Nils and Märta Schuberts fund. The phrase "Affibody molecule" is used in this publication instead of "Affibody® molecule."

REFERENCES

1. Hynes NE, Lane HA. ERBB receptors and cancer: the complexity of targeted inhibitors. *Nat Rev Cancer.* 2005;5:341–354.
2. Murphy CG, Modi S. HER2 breast cancer therapies: a review. *Biologics.* 2009;3: 289–301.
3. Harris L, Fritsche H, Mennel R, et al. American Society of Clinical Oncology 2007 update of recommendations for the use of tumor markers in breast cancer. *J Clin Oncol.* 2007;25:5287–5312.
4. Molina R, Barak V, van Dalen A. at al. Tumor markers in breast cancer: European Group on Tumor Markers recommendations. *Tumour Biol.* 2005;26: 281–293.
5. Zidan J, Dashkovsky I, Stayerman C, Basher W, Cozacov C, Hadary A. Comparison of HER-2 overexpression in primary breast cancer and metastatic sites and its effect on biological targeting therapy of metastatic disease. *Br J Cancer.* 2005;93:552–556.
6. Kenanova V, Wu AM. Tailoring antibodies for radionuclide delivery. *Expert Opin Drug Deliv.* 2006;3:53–70.
7. Tolmachev V. Imaging of HER-2 overexpression in tumors for guiding therapy. *Curr Pharm Des.* 2008;14:2999–3019.
8. Schmidt MM, Wittrup KD. A modeling analysis of the effects of molecular size and binding affinity on tumor targeting. *Mol Cancer Ther.* 2009;8:2861–2871.
9. Nord K, Nilsson J, Nilsson B, Uhlén M, Nygren P-Å. A combinatorial library of an α-helical bacterial receptor domain. *Protein Eng.* 1995;8:601–608.
10. Tolmachev V, Orlova A, Nilsson FY, et al. Affibody molecules: potential for in vivo imaging of molecular targets for cancer therapy. *Expert Opin Biol Ther.* 2007;7:555–568.
11. Orlova A, Magnusson M, Eriksson T, et al. Tumor imaging using a picomolar affinity HER2-binding Affibody molecule. *Cancer Res.* 2006;66:4339–4348.
12. Baum RP, Prasad V, Mv̈ller D, et al. Molecular imaging of HER2-expressing malignant tumors in breast cancer patients using synthetic ^{111}In- or ^{68}Ga-labeled Affibody molecules. *J Nucl Med.* 2010;51:892–897.
13. Jansson B, Uhlén M, Nygren PA. All individual domains of staphylococcal protein A show Fab binding. *FEMS Immunol Med Microbiol.* 1998;20:69–78.
14. Orlova A, Tolmachev V, Pehrson R, et al. Synthetic Affibody molecules: a novel class of affinity ligands for molecular imaging of HER2 expressing malignant tumors. *Cancer Res.* 2007;67:2178–2189.
15. Kramer-Marek G, Kiesewetter DO, Capala J. Changes in HER2 expression in breast cancer xenografts after therapy can be quantified using PET and ^{18}F-labeled Affibody molecules. *J Nucl Med.* 2009;50:1131–1139.
16. Orlova A, Wållberg H, Stone-Elander S, Tolmachev V. On the selection of a tracer for PET imaging of HER2-expressing tumors: direct comparison of a ^{124}I-labeled Affibody molecule and trastuzumab in a murine xenograft model. *J Nucl Med.* 2009;50:417–425.
17. McLarty K, Cornelissen B, Cai Z, et al. Micro-SPECT/CT with ^{111}In-DTPA-pertuzumab sensitively detects trastuzumab-mediated HER2 downregulation and tumor response in athymic mice bearing MDA-MB-361 human breast cancer xenografts. *J Nucl Med.* 2009;50:1340–1348.
18. Mume E, Orlova A, Nilsson F, et al. Evaluation of (4-hydroxyphenyl)ethyl) maleimide for site-specific radiobromination of anti-HER2 affibody. *Bioconjug Chem.* 2005;16:1547–1555.
19. Tolmachev V, Nilsson FY, Widström C, et al. ^{111}In-benzyl-DTPA-$Z_{HER2:342}$, an Affibody-based conjugate for in vivo imaging of HER2 expression in malignant tumors. *J Nucl Med.* 2006;47:846–853.
20. Orlova A, Tran T, Widström C, Engfeldt T, Eriksson Karlström A, Tolmachev V. Pre-clinical evaluation of [^{111}In]-benzyl-DOTA-$Z_{HER2:342}$, a potential agent for imaging of HER2 expression in malignant tumors. *Int J Mol Med.* 2007;20:397–404.
21. Ahlgren S, Orlova A, Rosik D, et al. Evaluation of maleimide derivative of DOTA for site-specific labeling of recombinant Affibody molecules. *Bioconjug Chem.* 2008;19:235–243.
22. Tolmachev V, Orlova A. Update on Affibody molecules for in vivo imaging of targets for cancer therapy. *Minerva Biotecnol.* 2009;21:21–30.
23. Feldwisch J, Tolmachev V, Lendel C, et al. Design of an optimized scaffold for Affibody molecules. *J Mol Biol.* 2010;398:232–247.
24. Lindmo T, Boven E, Cuttitta F, et al. Determination of the immunoreactive fraction of radiolabeled monoclonal antibodies by linear extrapolation to binding at infinite antigen excess. *J Immunol Methods.* 1984;72:77–89.
25. Engfeldt T, Tran T, Orlova A, et al. ^{99m}Tc-chelator engineering to improve tumor targeting properties of a HER2-specific Affibody molecule. *Eur J Nucl Med Mol Imaging.* 2007;34:1843–1853.
26. Ahlgren S, Wållberg H, Tran TA, et al. Targeting of HER2-expressing tumors with a site-specifically ^{99m}tc-labeled recombinant Affibody molecule, ZHER2: 2395, with C-terminally engineered cysteine. *J Nucl Med.* 2009;50:781–789.
27. Wållberg H, Orlova A. Slow internalization of anti-HER2 synthetic affibody monomer ^{111}In-DOTA-ZHER2:342-pep2: implications for development of labeled tracers. *Cancer Biother Radiopharm.* 2008;23:435–442.
28. Behr TM, Goldenberg DM, Becker W. Reducing the renal uptake of radiolabeled antibody fragments and peptides for diagnosis and therapy: present status, future prospects and limitations. *Eur J Nucl Med.* 1998;25:201–212.
29. Lub-de Hooge MN, Kosterink JG, Perik PJ, et al. Preclinical characterisation of ^{111}In-DTPA-trastuzumab. *Br J Pharmacol.* 2004;143:99–106.
30. Tang Y, Wang J, Scollard DA, et al. Imaging of HER2/neu-positive BT-474 human breast cancer xenografts in athymic mice using ^{111}In-trastuzumab (Herceptin) Fab fragments. *Nucl Med Biol.* 2005;32:51–58.
31. McLarty K, Cornelissen B, Scollard DA, Done SJ, Chun K, Reilly RM. Associations between the uptake of ^{111}In-DTPA-trastuzumab, HER2 density and response to trastuzumab (Herceptin) in athymic mice bearing subcutaneous human tumor xenografts. *Eur J Nucl Med Mol Imaging.* 2009;36:81–93.
32. Dijkers EC, Kosterink JG, Rademaker AP, et al. Clinical-grade ^{89}Zr-trastuzumab for HER2/neu ImmunoPET imaging. *J Nucl Med.* 2009;50:974–981.
33. Maeda H, Bharate GY, Daruwalla J. Polymeric drugs for efficient tumor-targeted drug delivery based on EPR-effect. *Eur J Pharm Biopharm.* 2009;71:409–419.